

# Coherent Supercontinuum Generation in Step-Index Heavily Ge-Doped Silica Fibers With All Normal Dispersion

Liang Chen , Meisong Liao, Wanjun Bi , Fei Yu , Tianxing Wang, Weiqing Gao, and Lili Hu 

**Abstract**—The step-index heavily germanium-doped silica fibers with all normal dispersion (ANDi) are promising candidates for highly coherent supercontinuum (SC). These ANDi step-index silica fibers are easier to fabricate, splice and handle than silica photonic crystal fibers (PCFs). 40% GeO<sub>2</sub> doped step-index silica fiber of 3 μm core diameter has flat and near-zero dispersion which is between −5.5 and 0 ps/nm/km from 1.4 to 2.4 μm. Highly coherent SC spanning from 1050 nm to 2100 nm generated from the ANDi step-index heavily germanium-doped silica fiber pumped at 1560 nm. All-fiber coherent SC source from 1200 nm to 2200 nm is achieved by splicing the ANDi silica fiber with a 1560 nm femtosecond fiber laser of 90% couple efficiency. Moreover, the step-index ANDi germania-core silica fiber of 2.2 μm core diameter is proposed to generate coherent mid-infrared SC from 1.7 to 3 μm. The ANDi step-index silica fibers not only can generate highly coherent broadband SC at near infrared or mid-infrared region but also can easily achieve all-fiber structure coherent SC source. And the experiment of supercontinuum generation in UNNA4 and UHNA7 fibers with different pump wavelengths indicates that the pump of 1064 nm is not suitable for coherent supercontinuum generation in the fiber of UNNA4 and UHNA7.

**Index Terms**—Supercontinuum, coherent, normal dispersion.

Manuscript received May 19, 2022; accepted May 20, 2022. Date of publication May 31, 2022; date of current version June 22, 2022. This work was supported in part by the National Key Research and Development Program of China under Grant 2018YFB0504500, in part by the National Natural Science Foundation of China under Grant 61905258, and in part by the Shanghai Professional Technical Public Service Platform of Advanced Optical Waveguide Intelligent Manufacturing and Testing under Grant 19DZ2294000. (Corresponding author: Meisong Liao.)

Liang Chen is with the The Key Laboratory of Material Science for High Power Laser, Shanghai Institute of Optics and Fine Mechanics, Chinese Academy of Sciences, Shanghai 201800, China, and also with the Center of Materials Science and Optoelectronics Engineering, University of Chinese Academy of Sciences, Beijing 100049, China (e-mail: chenliang01@siom.ac.cn).

Meisong Liao, Wanjun Bi, Fei Yu, and Tianxing Wang are with the The Key Laboratory of Material Science for High Power Laser, Shanghai Institute of Optics and Fine Mechanics, Chinese Academy of Sciences, Shanghai 201800, China (e-mail: liaomeisong@siom.ac.cn; biwanjun@siom.ac.cn; yufei@siom.ac.cn; wtx111000@gmail.com).

Weiqing Gao is with the School of Electronic Science and Applied Physics, Hefei University of Technology, Hefei 230009, China (e-mail: weiqinggao@yahoo.com).

Lili Hu is with the Hangzhou Institute for Advanced Study, University of Chinese Academy of Sciences, Hangzhou 310024, China (e-mail: hulili@siom.ac.cn).

Digital Object Identifier 10.1109/JPHOT.2022.3177945

## I. INTRODUCTION

**S**UPERCONTINUUM (SC) sources have been widely owing to its applications in pulse compression [1], [2], optical coherence tomography (OCT) [3], [4], optical frequency metrology [5], spectroscopy [6], laser confocal microscopy [7], and broadband fiber oscillator [8]. Coherence of the SC is one of important characteristic for these applications. Highly coherent SC increased the imaging penetration depth when it was applied in optical frequency metrology [9]. A frequency comb source pumped with highly coherent SC, which was used as the reference in the transmission experiment, resulted in negligible influence of bit error rate on phase shift keying transmission [10]. Generally, in order to generate broadband SC, the nonlinear fibers are pumped by femtosecond pulse in the anomalous dispersion regime [11]. In these cases, the broadening mechanisms of the SC are dominated by soliton fission or modulation instability, which increases the noise of the SC [12]. On the contrary, the all normal dispersion (ANDi) fiber is pumped to generate highly coherent SC, the broadening mechanisms in these cases are self-phase modulation (SPM) and optical wave-breaking (OWB) [13].

One approach to achieve ANDi has been reported in the silica photonic crystal fibers (PCFs). Heidt *et al.* fabricated ANDi silica PCFs, and coherent SC spanning the range from visible to near-infrared band was generated in the fibers [13]. Tarnowski *et al.* prepared ANDi microstructured silica fiber, and coherent SC up to 2.2 μm was obtained in the fibers [14]. Klimczak *et al.* proposed and drew all-solid soft-glass PCFs to achieve a normal dispersion profile flattened to within −50 to −30 ps/nm/km in the wavelength range of 1100 to 2700 nm, and coherent SC spanning from 930 nm to 2170 nm with spectral flatness of 7 dB was generated from the fibers [15]. Although the PCFs exhibit flexible dispersion adjustment capability to achieve ANDi, the preparation of the fibers is complex and the fibers are hard to handle comparing to the step-index fibers.

Recently, the step-index fibers with high numerical aperture (NA) were fabricated to achieve ANDi to generate coherent SC. Saini *et al.* demonstrated highly coherent mid-infrared SC in the ANDi step-index tellurite fiber, the NA of the fiber is 0.607 at 2 μm [16]. Strutyński *et al.* fabricated a step-index tellurite fiber with NA of 0.7 to achieve ANDi [17]. These tellurite fibers have sufficient big refractive index differences to confine the mode and tailor the dispersion of the fiber when the core diameter of

the fibers are  $3.5 \mu\text{m}$  or smaller. Owing to the good transmission in the mid-infrared region, these fibers are promising candidates for coherent mid-infrared SC. For visible to near infrared SC generation, silica or silicate fibers are more suitable owing to higher fiber strength and low splicing loss comparing to that of the tellurite fibers. Step-index heavily germanium-doped silica fibers are fabricated by doping high content  $\text{GeO}_2$  into the silica core, which not only can provide big refractive index difference, but also can increase the nonlinear of the fiber. So, the step-index heavily germanium-doped silica fibers are promising nonlinear mediums to achieve ANDi to generate coherent SC. Reddy *et al.* report the fabrication, characterization, and broadband supercontinuum generation of ultra-high numerical-aperture heavily (50 mol. %)  $\text{GeO}_2$ -doped optical fiber [18].

There are some demonstrations of the step-index heavily germanium-doped silica fibers for SC generation. For example, commercially available ultra-high numerical aperture (UHNA) fibers manufactured by Nufern, which dope  $\text{GeO}_2$  into the silica core, have ANDi up to  $2.4 \mu\text{m}$ . The spectral interferometry technique was used to measure the dispersion of the fibers (UHNA1, UHNA3, UHNA4, UHNA7, and PM2000D) [19]. Owing to the small core and ANDi of these fibers, SC generation for optical coherence tomography has been demonstrated in these fibers [20], [21]. However, the spectral widths of the SC are 300 nm or less in these demonstrations. Highly coherent broadband SC has not been reported in these fibers. In addition, owing to lower loss at 2-3  $\mu\text{m}$  compared to silica fiber, the step-index heavily germanium-doped silica fibers are attractive options for mid-infrared SC generation recently. Most demonstrations focus on generating broadband SC extending to mid-infrared region [22]–[24]. Also, highly coherent mid-infrared SC has not been proposed in these fibers. In short, step-index heavily germanium-doped silica fibers are potential nonlinear medium to achieve ANDi, highly coherent broadband SC are promising to generate from these fibers.

In this work, dispersion of the step-index heavily germanium-doped silica fibers are investigated. The SC generation are explored in the ANDi step-index heavily germanium-doped silica fibers (UHNA4 and UHNA7 from Coherent-Nufern). Highly coherent broadband SC spanning from 1050 nm to 2100 nm generated from the UHNA7 pumped with a femtosecond fiber laser at 1560 nm. Also, All-fiber coherent SC sources from 1200 to 2200 were achieved by splicing UHNA7 with a femtosecond fiber laser. The step-index pure germania core silica fibers are proposed to generate highly coherent mid-infrared SC spanning from 1700 nm to 3000 nm. The investigation in this paper shows that the step-index heavily germanium-doped silica fibers are promising candidates for highly coherent SC generation owing to advantages of fabricating, splicing and handling.

## II. SIMULATIONS AND EXPERIMENTS

The step-index heavily germanium-doped silica fibers are fabricated by doping high content  $\text{GeO}_2$  into the silica core, and  $\text{GeO}_2$  doped silica fibers with concentration varying from 30 mol % to 100 mol % have been demonstrated [22], [23], [25], so any concentration of  $\text{GeO}_2$  doped silica fiber core can be prepared

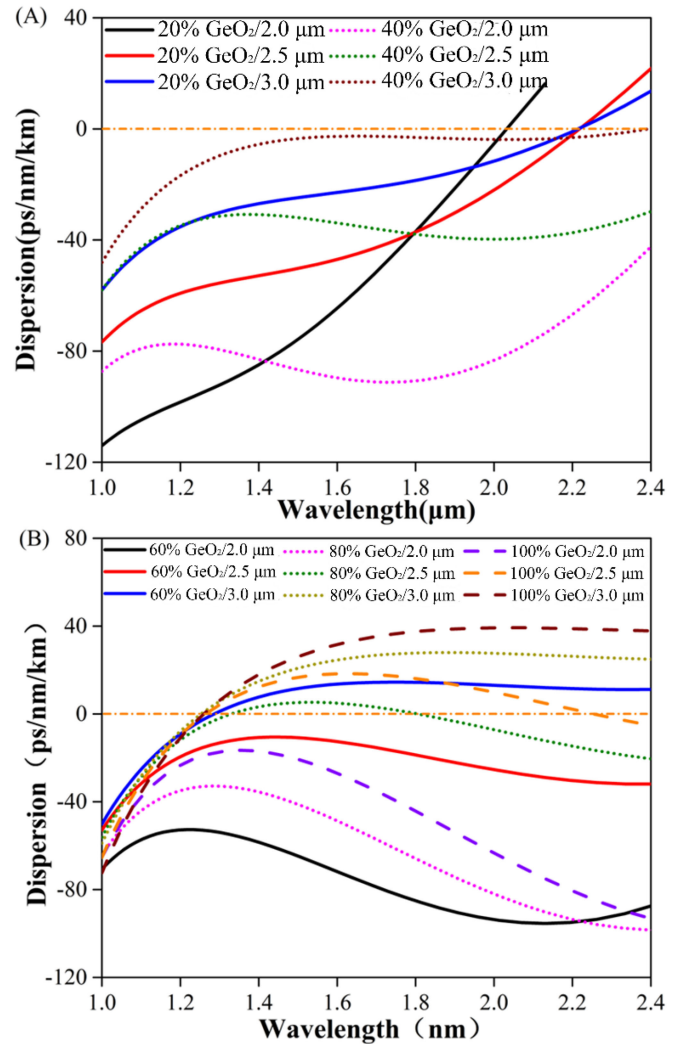


Fig. 1. Calculated dispersion of the  $\text{GeO}_2$  doped silica fibers with diameter of the core varying from 2 to 3  $\mu\text{m}$ .  $\text{GeO}_2$  doped content (A) 20% and 40% (B) 60%, 80% and 100%.

in theory. The pure germania-core silica fibers are regarded as 100 mol %  $\text{GeO}_2$  doped silica fibers in this work.  $\text{GeO}_2$  doped silica fibers with various concentrations supply enough large refractive index difference, which can achieve ANDi in the fiber with small core. Fig. 1 shows the calculated dispersion of the  $\text{GeO}_2$  doped silica fibers with concentration varying from 20% to 100% (mol%) and diameter of the core varying from 2 to 3  $\mu\text{m}$  by Finite Element Method (FEM). The Sellmeier coefficients of  $\text{GeO}_2$ -doped silica are obtained from the ref. [26].

The results show that the silica fiber is not ANDi up to  $2.4 \mu\text{m}$  with 20%  $\text{GeO}_2$  doped. The reason is that the difference of refractive indices between core and cladding is not large enough to confine the mode at long wavelength region. 40% or more than 40%  $\text{GeO}_2$  doped silica fibers can achieve ANDi up to  $2.4 \mu\text{m}$ . Although all these fibers are capable of achieving ANDi, the value and flatness of the dispersion are different owing to various  $\text{GeO}_2$  doped concentrations. For the same  $\text{GeO}_2$  doped content, the dispersion of the fiber becomes more flat with diameter of the core increasing from 2 to 3  $\mu\text{m}$ . When the  $\text{GeO}_2$  doped

TABLE I  
THE PARAMETERS OF UHNA4 AND UHNA7

	Cutoff wavelength (nm)	Mode field diameter ( $\mu\text{m}$ ) @1550 nm	Ge-concentration	Core NA
UHNA4	1050	4	~30%	0.35
UHNA7	1450	3.2	~40%	0.41

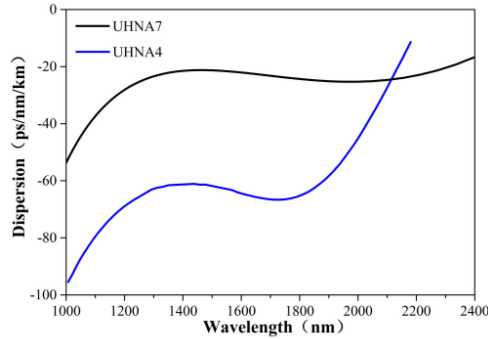


Fig. 2. Dispersion profiles of the UHNA4 and UHNA7.

content increases from 40% to 100%, smaller diameter of the core is required to achieve ANDi between 1 and 2.4  $\mu\text{m}$ . So, when  $\text{GeO}_2$  doped concentration increasing from 40% to 100%, the ANDi fiber has steeper dispersion, which is unfavorable for broadening of SC at normal dispersion region. As shown in the Fig. 1(a), 40%  $\text{GeO}_2$  doped silica fiber with 3  $\mu\text{m}$  core diameter has the flattest dispersion between -5.5 and 0 ps/nm/km from 1.4 to 2.4  $\mu\text{m}$ , and the fiber is the most suitable nonlinear medium to generate coherent SC between 1 to 2.4  $\mu\text{m}$  from the perspective of fiber dispersion. Due to limited experimental conditions, the 40%  $\text{GeO}_2$  doped silica fiber with 3  $\mu\text{m}$  core diameter cannot be fabricated by our research group. So, ANDi commercial UHNA silica fibers, which are also heavily germanium-doped silica fibers, instead to act as nonlinear medium to generate coherent SC.

UHNA4 and UHNA7 are ANDi heavily germanium-doped silica fibers supplied by Coherent-Nufern. The NA of the UHNA4 and UHNA7 are 0.35 and 0.41, respectively. The corresponding  $\text{GeO}_2$  doped content of UHNA4 and UHNA7 are about 30% and 40%, which are not given by Coherent-Nufern. The core diameter of the UHNA4 and UHNA7 are 2.2  $\mu\text{m}$  and 2.4  $\mu\text{m}$ , respectively, as shown in Table I.

Fig. 2 shows the dispersion profiles of the UHNA4 and UHNA7 [17]. For the UHNA7, the dispersion fluctuation of the fiber is within  $\pm 5$  ps/nm/km spanning from 1250 to 2200 nm, which is beneficial for the OWB initiated four wave mixing (FWM) during SC broadening [27]. For the UHNA4, absolute value and slope of the dispersion are larger than those of the UHNA7, and ANDi of the fiber is just up to 2300 nm. So, the UHNA 7 are more suitable compared to UHNA 4 to generate coherent broadband SC. Next, the experiments of generating SC in these fibers are introduced.

In order to investigate the process and coherence of the SC in the fibers, both the experiments and numerical simulations are performed.

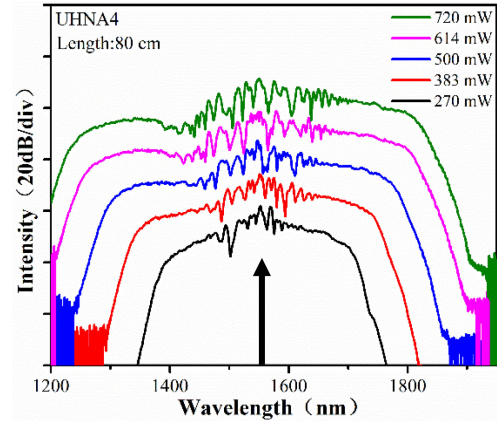


Fig. 3. Power-dependent SC spectrum measured in the UHNA4 pumped by a 1560 nm (black arrow) femtosecond fiber laser.

UHNA 4 and UHNA 7 are pumped by a 1560 nm femtosecond fiber laser (Carmel Model CLF-10CFF), which provides 88 fs pulses with a repetition rate of 80 MHz, a maximum average power of 2.26 W. The laser was coupled into the fibers by a mounted aspheric lens (Thorlabs, N414TM-C) with focal length of 3.3 mm and NA of 0.47. The length of UHNA 4 and UHNA 7 both are 80 cm, and the spectrometers (Yokogawa) are used to measure the spectra from the fibers by a silica fiber cable, and the power meters (Thorlabs, S401C and PM100D) are used to measure the power.

Fig. 3 shows the spectrum of SC from the UHNA 4 pumped at 1560 nm for various pumping power. The SC broadens almost symmetrically around the pump wavelength with increasing pumping power. This indicates that the broadening mechanism of the SC is dominated by SPM and OWB [13]. The SC spanning from 1200 to 1900 nm generates in the step-index silica fiber with the highest average power of 720 mW. The coupling efficiency which defined as the ratio of the power output from the fiber to the power before being focused into the fiber by the lens is about 32% without fiber loss in consideration.

Fig. 4 shows the spectrum of SC from the UHNA 7 pumped at 1560 nm with various pumping power. Also, the spectrum of the SC broadens symmetrically when the power of the SC increases from 230 to 586 mW. The SC spanning from 1000 to 2150 nm generates in the fiber with the pumping power increasing to 2.26 W. The coupling efficiency of the UHNA 7 is 26%, which is a little lower than the coupling efficiency of UHNA 4. However, SC of 586 mW in the UHNA 7 is wider than that of 720 mW in the UHNA 4. Owing to bigger NA of UHNA 7, the mode field diameter of the UHNA 7 is 3.2  $\mu\text{m}$  at 1560 nm, which is smaller than that of UHNA 4 whose is 4  $\mu\text{m}$  at 1560 nm. In addition, the nonlinear refraction of UHNA7 is stronger



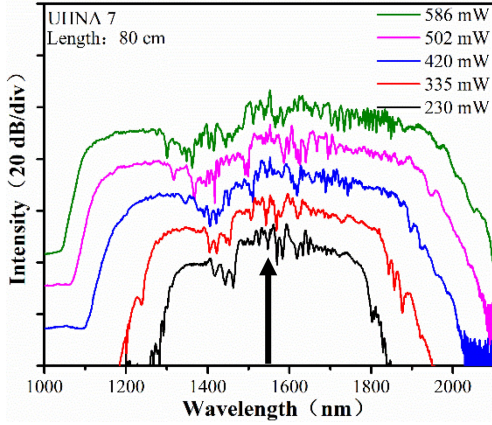


Fig. 4. Power-dependent SC spectrum measured in the UHNA7 pumped by a 1560 nm (black arrow) femtosecond fiber laser.

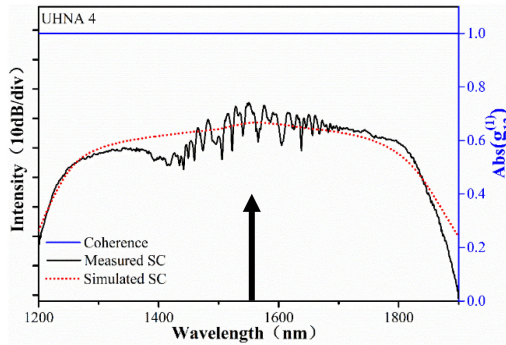


Fig. 5. Simulated and measured SC spectrum at output power of 720 mW in the UHNA 4, and calculated coherence of the SC with 1560 nm (black arrow) pumped.

than that of UHNA 4 due to higher doped  $\text{GeO}_2$ . Therefore, the nonlinear coefficient of UHNA7 is about 1.6 times that of UHNA 4. Also, the dispersion of UHNA 7 is flatter than that of UHNA 4. In short, due to higher nonlinear coefficient and flatter dispersion, UHNA 7 is more suitable than UHNA 4 for generating of coherent broadband SC.

In order to investigate coherence of the SC, the generalized nonlinear Schrödinger equation is used to simulate the SC in UHNA 4 and UHNA 7. The parameters of the pump pulse and the dispersion of the fibers used in the simulations are mentioned above, and the parameters of Raman response are used as the same as silica. The coherence of the SC is calculated with random noise seeds for 108 times. The degree of coherence is given by the  $|g_{12}^{(1)}|$  according to the process explained in ref. [28], which is used to evaluate the consistency of spectra and phase between different pulses of the supercontinuum.  $|g_{12}^{(1)}|$  gives a positive number in the interval [0:1] with the value of 1 representing perfect coherence. The highly coherent supercontinuum refer to that the value of  $|g_{12}^{(1)}|$  is approximate 1. Fig. 5 shows the simulated and measured SC in the UHNA 4, and the calculated coherence of the SC. The simulated SC agrees well with the measured SC whose average power is 720 mW. The results demonstrate that the set parameters are appropriate. In the region of the generated SC, the  $|g_{12}^{(1)}|$  of SC is 1, which indicates

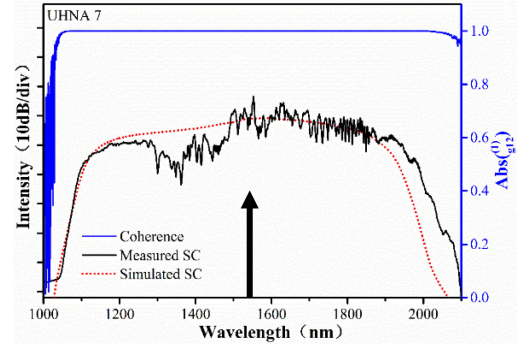


Fig. 6. Simulated and measured SC spectrum at output power of 586 mW in the UHNA 7, and calculated coherence of the SC with 1560 nm (black arrow) pumped.

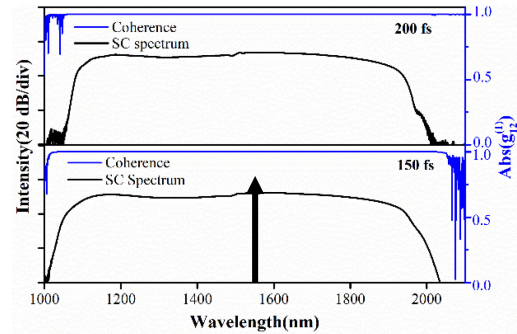


Fig. 7. Spectrum and coherences of the SC with pumping pulse widths of 150 fs and 200 fs of 1560 nm (black arrow).

the SC is highly coherent. The reason is that the broadening mechanism of the SC is mainly dominated by SPM. Fig. 6 shows simulated and measured SC in the UHNA 7, and the calculated coherence of the SC. Also, the simulated SC agrees with the measured SC whose average power is 586 mW. The calculated  $|g_{12}^{(1)}|$  of SC is about 1 at the range from 1050 to 2050 nm, which corresponds to highly coherent SC owing to SPM and OWB. The results show that ANDi UHNA fibers can generate highly coherent broadband SC. Although these results are comparable with the coherent SC generated from the silica or silicate PCFs which were pumped at 1560 nm, the step-index silica fibers are easier to fabricate, splice and handle. So, the step-index ANDi heavily germanium-doped silica fibers are promising candidates for highly coherent SC, especially 1  $\mu\text{m}$  to 2  $\mu\text{m}$ .

Going one step further, the coherences and spectra of the SC generated from the UHNA 7 are calculated when pulse durations are 150 fs and 200 fs. The peak power of the pulses is fixed to 100 kW, and other parameters of the simulations are same as mentioned above. The simulation results are shown in the Fig. 7. The SC from 1000 to 2000 nm generate from the fiber, and the calculated  $|g_{12}^{(1)}|$  of SC are about 1 when the pulse widths are 150 fs and 200 fs. It is clear that the SC is also highly coherent when the pulse duration is over 100 fs. The fiber lasers with pulse durations over 100 fs are cheap and easy to achieve, so the UHNA 7 is potential candidate for all-fiber coherent SC source.

Then, all-fiber coherent SC source is achieved by splicing the UHNA 7 with a 1560 nm femtosecond laser. The laser provides 140 fs pulse with a repetition rate of 50 MHz. The fiber

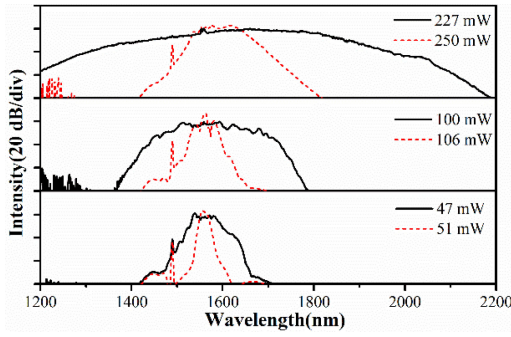


Fig. 8. The output spectrum of the 1560 nm femtosecond fiber laser at various output powers of 51 mW, 106 mW and 250 mW (red dash line), and the corresponding output SC spectrum of 1 m long UHNA 7 with different average power of 47 mW, 100 mW and 227 mW (black solid line).

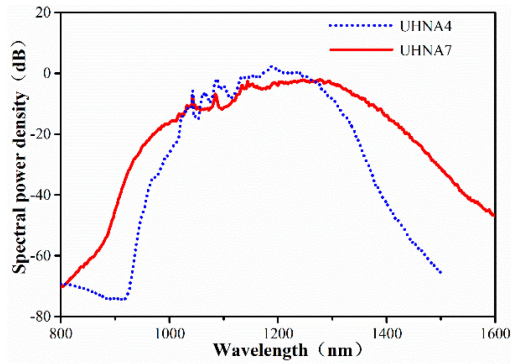


Fig. 9. SC spectra in the 80 cm long UHNA 4 and UHNA 7 pumped at 1064 nm.

at output of the laser is SMF-28 (8/125  $\mu\text{m}$ ), and the UHNA 7 (2.4/125  $\mu\text{m}$ ) is directly spliced to the fiber. Fig. 8 shows output spectrum of SMF-28 at various output powers of 51 mW, 106 mW and 250 mW (red dash lines), and the corresponding output SC spectrum of 1 m long UHNA 7 at different output powers of 47 mW, 100 mW and 227 mW (black solid line). The results show that the all-fiber SC spanning from the 1200 to 2200 nm generates from the UHNA 7 when the pump power is 250 mW. Also, the results illustrate that the SC spectrum broaden symmetrically, which indicates the main broadening mechanism is SPM. So, the all-fiber SC are highly coherent. In addition, couple efficiency of the UHNA 7 and SMF-28 is about 91%, which is more than three times that of the spatial coupling. The all-fiber coherent SC source not only has high couple efficiency but also is not susceptible to vibrations, which is favorable for the applications of the coherent SC source under complex environment. The results indicate that the ANDi step-index heavily germanium-doped silica fibers are promising nonlinear mediums to achieve all-fiber coherent SC source.

In order to compare the SC generation in the ANDi UHNA fibers pumped at different wavelength, the UHNA 4 and UHNA 7 are also pumped at 1064 nm by a femtosecond fiber laser with pulse width of 50 fs, repetition rate of 80 MHz and average power of 2.2 W to generate SC. The length of fibers, lens and spectrometer are same as mentioned above. Fig. 9 shows the SC spectra in 80 cm long UHNA 4 and UHNA 7 pumped at 1064 nm. The SC spanning from 900 nm to 1500 nm generates

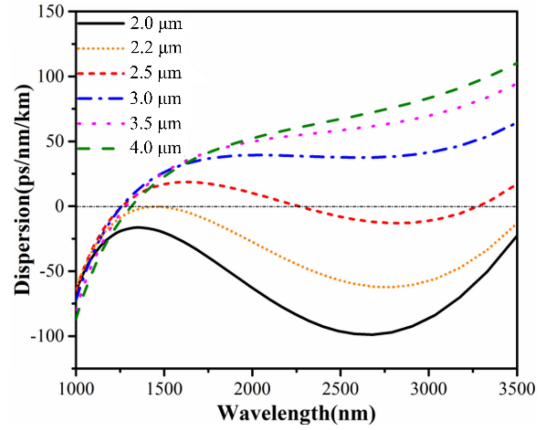


Fig. 10. Calculated dispersion of the pure germania core silica fiber with diameter of the core varying from 2 to 4  $\mu\text{m}$ .

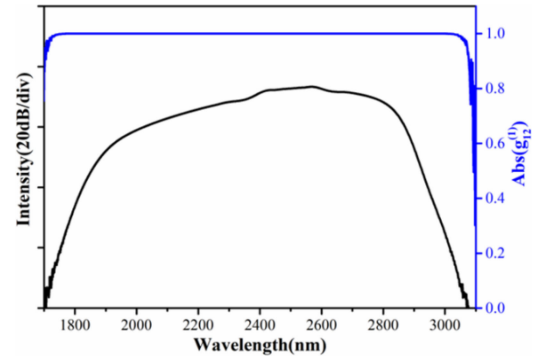


Fig. 11. Simulated spectrum and coherence of the SC from the pure germania core silica fiber.

in the UHNA 4, and the average power of the SC is 1.39 W. Although the coupling efficiency is 63%, the width of SC is just 600 nm and the spectrum is not symmetrical. The reason is that the dispersion of fiber is smaller and flatter at the long wavelength region than that at short wavelength region. Also, the SC spanning from 800 to 1600 nm generated in the UHNA 7 is not symmetrical, and the width of red-shifted SC is twice that of blue-shifted SC. So, comparing to the silica PCFs [13], [29], [30], these fibers are not suitable for coherent SC pumped at 1064 nm.

In this section, pure germania core silica fibers are proposed to generate highly coherent mid-infrared SC. The GeO<sub>2</sub> not only has high nonlinear refractive index of  $9.5 \times 10^{-20} \text{ m}^2 \text{ W}^{-1}$  but also good transmission in mid-infrared region. Fig. 10 shows the dispersion of the fiber with different core diameters. With decreasing of the core diameter, the dispersion of the fiber decreases between 1500 and 3500 nm. When the core diameter of the fiber is 2.2  $\mu\text{m}$  or less than 2.2  $\mu\text{m}$ , ANDi can be achieved from 1000 to 3500 nm. The fiber with core diameter of 2.2  $\mu\text{m}$  is selected to generate highly coherent mid-infrared SC.

The generalized nonlinear Schrödinger equation is used to simulate the spectrum and coherence of the SC. The width and peaking power of the pumping pulse is 150 fs and 50 kW, respectively. The length of the fiber is set as 5 cm, and the fiber is pumped at 2500 nm. The loss of the fiber between



1000 to 3000 nm is not in consideration because of short length of the fiber according to ref. [22]. Fig. 11 shows that the SC spanning from 1700 to 3000 nm generates from 5 cm long fiber. The calculated  $|g_{12}^{(1)}|$  of SC is 1 from 1700 to 3000 nm, which indicates the SC is highly coherent. The results show that the pure germania core silica fiber of 2.2  $\mu\text{m}$  core diameter is a promising candidate for mid-infrared highly coherent SC, especially 2 to 3  $\mu\text{m}$ .

### III. CONCLUSION

In this work, the ANDi step-index heavily germanium-doped silica fibers are used as nonlinear mediums to generate coherent SC. The dispersion of the fibers with various  $\text{GeO}_2$  doped concentration and core diameter are investigated, and 40%  $\text{GeO}_2$  doped silica fiber of 3  $\mu\text{m}$  core diameter has the flattest and near-zero ANDi which is between -5.5 and 0 ps/nm/km from 1.4 to 2.4  $\mu\text{m}$ . Highly coherent SC spanning from 1050 nm to 2100 nm generates from the UHNA 7. Also, all-fiber coherent SC spanning from 1200 to 2200 nm is achieved by splicing the UHNA 7 and the 1560 nm femtosecond fiber laser of 90% couple efficiency. The experiment of SC generation in UNNA4 and UHNA7 fibers with different pump wavelengths also indicates that the pump of 1064 nm is not suitable for coherent SC generation in the fiber of UNNA4 and UHNA7. Finally, the pure germania core silica fiber of 2.2  $\mu\text{m}$  core diameter is proposed to generate highly coherent mid-infrared SC from 1700 to 3000 nm. So, the step-index heavily germanium-doped silica fibers are promising candidates for highly coherent SC generation owing to advantages of fabricating, splicing and handling.

### DISCLOSURES

The authors declare no conflicts of interest.

### REFERENCES

- [1] B. Schenkel, R. Paschotta, and U. Keller, "Pulse compression with supercontinuum generation in microstructure fibers," *J. Opt. Soc. Amer. B*, vol. 22, no. 3, pp. 687–693, 2005.
- [2] A. M. Heidt *et al.*, "High quality sub-two cycle pulses from compression of supercontinuum generated in all-normal dispersion photonic crystal fiber," *Opt. Exp.*, vol. 19, no. 15, pp. 13873–13879, 2011.
- [3] S. Moon and D. Y. Kim, "Ultra-high-speed optical coherence tomography with a stretched pulse supercontinuum source," *Opt. Exp.*, vol. 14, no. 24, pp. 11575–11584, 2006.
- [4] E. W. Chang, R. Su, S. H. Yun, E. Sergeeva, M. Kirillin, and L. Mattsson, "Perspectives of mid-infrared optical coherence tomography for inspection and micrometrology of industrial ceramics," *Opt. Exp.*, vol. 22, no. 13, pp. 15804–15819, 2014.
- [5] A. Schliesser, N. Picqué, and T. W. Hänsch, "Mid-infrared frequency combs," *Nature Photon.*, vol. 6, no. 7, pp. 440–449, 2012.
- [6] P. S. Johnston and K. K. Lehmann, "Cavity enhanced absorption spectroscopy using a broadband prism cavity and a supercontinuum source," *Opt. Exp.*, vol. 16, no. 19, pp. 15013–15023, 2008.
- [7] K. Lindford, T. Kalkbrenner, and P. Stoller, "Detection and spectroscopy of gold nanoparticles using supercontinuum white light confocal microscopy," *Phys. Rev. Lett.*, vol. 93, no. 3, 2004, Art. no. 037401.
- [8] Y. Guo, X. Li, P. Guo, and H. Zheng, "Supercontinuum generation in an Er-doped figure-eight passively mode-locked fiber laser," *Opt. Exp.*, vol. 26, no. 8, 2018, Art. no. 9893.
- [9] H. Kawagoe *et al.*, "Development of a high power supercontinuum source in the 17  $\mu\text{m}$  wavelength region for highly penetrative ultrahigh-resolution optical coherence tomography," *Biomed. Opt. Exp.*, vol. 5, no. 3, 2014, Art. no. 932.
- [10] C. B. Huang, S. G. Park, D. E. Leaird, and A. M. Weiner, "Nonlinearly broadened phase-modulated continuous-wave laser frequency combs characterized using DPSK decoding," *Opt. Exp.*, vol. 16, no. 4, 2008, Art. no. 2520.
- [11] G. P. Agrawal, *Nonlinear Fiber Optics*, 5th ed., Oxford, UK; Waltham, MA, USA: Academic Press, 2013.
- [12] J. Swiderski, "High-power mid-infrared supercontinuum sources: Current status and future perspectives," *Prog. Quantum Electron.*, vol. 38, no. 5, pp. 189–235, 2014.
- [13] A. M. Heidt *et al.*, "Coherent octave spanning near-infrared and visible supercontinuum generation in all-normal dispersion photonic crystal fibers," *Opt. Exp.*, vol. 19, no. 4, 2011, Art. no. 3775.
- [14] K. Tarnowski, T. Martynkien, A. Anuszkiewicz, P. Mergo, and K. Poturaj, "Coherent supercontinuum generation beyond 2.6  $\mu\text{m}$  in all-normal dispersion silica microstructured fibers," *Opt. Exp.*, vol. 24179, no. 2014, 2016, Art. no. 7100311.
- [15] M. Klimczak *et al.*, "Coherent supercontinuum generation up to 23  $\mu\text{m}$  in all-solid soft-glass photonic crystal fibers with flat all-normal dispersion," *Opt. Exp.*, vol. 22, no. 15, pp. 18824–18832, 2014.
- [16] T. S. Saini *et al.*, "Coherent mid-infrared supercontinuum spectrum using a step-index tellurite fiber with all-normal dispersion," *Appl. Phys. Exp.*, vol. 11, 2018, Art. no. 102501.
- [17] C. Strutyński *et al.*, "Tailoring supercontinuum generation beyond 2  $\mu\text{m}$  in step-index tellurite fibers," *Opt. Lett.*, vol. 42, no. 2, pp. 247–250, 2017.
- [18] P. H. Reddy *et al.*, "Fabrication of ultra-high numerical aperture  $\text{GeO}_2$ -doped fiber and its use for broadband supercontinuum generation," *Appl. Opt.*, vol. 56, no. 33, pp. 9315–9324, 2017.
- [19] P. Ciącka, A. Rampur, A. Heidt, T. Feurer, and M. Klimczak, "Dispersion measurement of ultra-high numerical aperture fibers covering thulium, holmium, and erbium emission wavelengths," *J. Opt. Soc. Amer. B*, vol. 35, no. 6, pp. 1301–1307, 2018.
- [20] D. L. Marks, A. L. Oldenburg, J. J. Reynolds, and S. A. Boppart, "Study of an ultrahigh-numerical-aperture fiber continuum generation source for optical coherence tomography," *Opt. Lett.*, vol. 27, no. 22, 2007, Art. no. 2010.
- [21] N. Nishizawa, Y. Chen, P. Hsiung, V. Sharma, T. H. Ko, and J. G. Fujimoto, "All fiber high resolution OCT system using an ultrashort pulse high power fiber laser," in *Proc. Conf. Lasers Electro-Opt./Int. Quantum Electron. Conf. Photonic Appl. Syst. Technol. Tech.*, 2004, vol. 1, p. 2.
- [22] G. Liu, L. Yang, J. Yao, K. Yin, B. Zhang, and J. Hou, "06–32  $\mu\text{m}$  supercontinuum generation in a step-index germania-core fiber using a 44 kW peak-power pump laser," *Opt. Exp.*, vol. 24, no. 12, 2016, Art. no. 12600.
- [23] D. J. Ain *et al.*, "Scaling power, bandwidth, and efficiency of mid-infrared supercontinuum source based on a  $\text{GeO}_2$ -doped silica fiber," *J. Opt. Soc. Amer. B*, vol. 36, no. 2, pp. 86–92, 2019.
- [24] E. A. Anashkina, A. V. Andrianov, M. Y. Koptev, S. V. Muravyev, and A. V. Kim, "Towards mid-infrared supercontinuum generation with germano-silicate fibers," *IEEE J. Sel. Top. Quantum Electron.*, vol. 20, no. 5, pp. 643–650, Sep./Oct. 2014.
- [25] R. Sidharthan, D. Jain, O. Bang, S. Yoo, D. Ho, and P. M. Moselund, "Record power, ultra-broadband supercontinuum source based on highly  $\text{GeO}_2$  doped silica fiber," *Opt. Exp.*, vol. 24, no. 23, 2016, Art. no. 26667.
- [26] J. W. Fleming, "Dispersion in  $\text{GeO}_2$ - $\text{SiO}_2$  glasses," *Appl. Opt.*, vol. 23, no. 24, 1984, Art. no. 4486.
- [27] M. Klimczak, B. Siwicki, A. Heidt, and R. Buczyński, "Coherent supercontinuum generation in soft glass photonic crystal fibers," *Photon. Res.*, vol. 5, no. 6, pp. 710–727, 2017.
- [28] A. M. Heidt, "Pulse preserving flat-top supercontinuum generation in all-normal dispersion photonic crystal fiber," *J. Opt. Soc. Amer. B*, vol. 27, no. 3, pp. 550–559, 2010.
- [29] I. A. Sukhoivanov, S. O. Iakushev, O. V. Shulika, J. A. Andrade-Lucio, A. Díez, and M. Andrés, "Supercontinuum generation at 800 nm in all-normal dispersion photonic crystal fiber," *Opt. Exp.*, vol. 22, no. 24, pp. 30234–30250, 2014.
- [30] L. E. Hooper, P. J. Mosley, A. C. Muir, W. J. Wadsworth, and J. C. Knight, "Supercontinuum generation in photonic crystal fiber with all-normal group velocity dispersion," *Opt. Exp.*, vol. 19, no. 6, pp. 4902–4907, 2011.